www.czasopisma.pan.pl PAN www.journals.pan.pl
POLSKA AKADEMIA NAUK

JOURNAL OF WATER AND LAND DEVELOPMENT
e-ISSN 2083-4535

Polish Academy of Sciences (PAN), Committee on Agronomic Sciences
Section of Land Reclamation and Environmental Engineering in Agriculture
Institute of Technology and Life Sciences (ITP)

JOURNAL OF WATER AND LAND DEVELOPMENT
2020, No. 46 (VII–IX): 1–9
https://doi.org/10.24425/jwld.2020.134083

Available (PDF): http://www.itp.edu.pl/wydawnictwo/journal; http://journals.pan.pl/jwld

Received 03.12.2019
Reviewed 09.04.2020
Accepted 14.04.2020

The coefficient of head loss at the pipe bend 90° with the sliced bend

Moh ABDUH[1)] ✉, Suhardjono SUHARDJONO[2)], Sumiadi SUMIADI[2)], Very DERMAWAN[2)]

[1)] Universitas Muhammadiyah Malang, Department of Civil Engineering, Jalan Raya Tlogomas 246 Malang, 65145, East Java, Indonesia
[2)] Universitas Brawijaya, Malang East Java, Indonesia

For citation: Abduh M., Suhardjono S., Sumiadi S., Dermawan V. 2020. The coefficient of head loss at the pipe bend 90° with the sliced bend. Journal of Water and Land Development. No. 46 (VII–IX) p. 1–9. DOI: 10.24425/jwld.2020.134083.

Abstract

The head loss is a decrease in compressive height caused by friction and direction changes of flow at the sliced bend. This method expected to provide is easy, fast, and economical. The elements of influence are the velocity of flow, the number of slices, average length of sliced walls, angle changes of the sliced, coefficient of friction, acceleration of gravity, and slope of the pipe. Equation for coefficient of head loss (K_b) is an analysis method for the head loss (hL) calculation. The analysis results that have obtained are the larger diameter of the pipe, and the more slices with a fixed discharge, the coefficient of hL becomes small. Conversely, if the diameter of the pipe is getting smaller, and the slice is getting less, then the coefficient of hL becomes bigger. This method, expected to give new knowledge in pipeline network applications, especially for the large diameter of pipelines.

Key words: *direction change, head loss, loss coefficient, pipeline network, sliced bend, slice numbers*

INTRODUCTION

As one of the infrastructures needed by the community to support daily life, the pipeline network serves as a means of transportation of fuel, both liquid, gas, and freshwater. The function of the piping network being adequate if each pipe has been assembled into one system and forms a network. These necessary to connect each part using a connecting device, one of which is a bend. These connections throughout the trip caused the head loss of bends.

This research aims to obtain an effective and efficient method in the design of head loss in bend and could use as a scientific basis in supporting field implementation. With the 90° sliced bend, the application in the field more efficient, both in terms of time and cost, so that it can contribute to development, especially in the pipeline network.

The head loss analysis of bends generally uses the curved bend, but the implementation of the field often by sliced bend, especially in large diameter of pipes (as steel pipe and HDPE). Based on the literature studies and previous research about two models of bend, the result of head loss is different, therefore need further research to get a suitable equation for the head loss of sliced bends. The hypothesis used in the analysis is due to friction and direction changes of the flow.

The pressure variation on the inner surface was complicated, the velocity must decrease when approaching the bend so that the safety of the pipe is maintained. It is the theoretical basis for the examination of the structural design of bends [LU *et al.* 2015]; the curved bend has difficulty in measure for head loss. There is no theoretically reliable method for predicting head loss [SPEDDING *et al.* 2008], the head loss coefficient generally shows a decreasing trend due to Reynolds numbers for certain angle and pipe diameter [ISLAM *et al.* 2016].

Study on turbulent flow with LES and RANS method, the flow field in bend is asymmetrical, intensity and the pattern of the vortex change over time in small scale, and induce the asymmetry of the flow field [WANG *et al.* 2016]. The velocity profile at the inner core of the pipe bend tries to recover if Re increases. If Re not increased, the separation point moved towards the upstream, and the reattachment point moved downstream of the bend [DUTTA *et al.* 2016]. The decrease of the hL is affected by fraction

of each phase which is directly related to the fluid density [WAHYUDI *et al*. 2016], the inside of the upstream bends caused disturbances so that the fluid velocity at the downstream was not ideal, and had a significant effect on the accuracy of the measurements [ZHANG *et al*. 2018].

Parametric model of a double bends 90°, with CFD tool for analysis of flow fields, velocity was seen to be higher at downstream due to the change in bend shape and high momentum [ADJEI, MOHSIN 2014], two types of flow are considered, flow under condition of maximum flow and flow under maximum velocity respectively [ZEGHADNIA *et al.* 2015]. The flow exhibits very complicated characteristics significantly. The pressure difference among the entrance and exit of the bend is significant on the outside wall [SUMIDA, SENOO 2015].

The secondary motions formed downstream of a 90° bend appear principally by two swirl motions [HELLSTRÖM *et al*. 2013]. The swirl intensity of secondary flow, the *R*:*D* of the bend a dominant function and Re function a weakly. However, additional studies are required to provide a correlation between swirl intensity and *R*:*D* [KIM *et al*. 2014]; [DUTTA, NANDI 2015a]. The bends having a small *R*:*D*, adds significant head loss, and this tends to constant for higher *R*:*D*. Additional studies are necessary to provide a correlation between the head loss coefficient and the *R*:*D* [DUTTA, NANDI 2015b].

The curved pipe is an example of cross-stream secondary motions induced by the geometry and centrifugal forces. Dean vortices associated with the motion of the particles show that these are moved towards the side-walls and are more intense than those of the mean flow [NOORANI *et al.* 2015]. The value of the head loss coefficient varies inversely with the *R*:*D* at curved bends. Further research is needed to provide results beyond the *R*:*D* range [CHOWDHURY *et al.* 2016]. Flow changes and velocity distribution occur due to the influence of the guide on the 90° bend pipe [KUMAR SAHA, NANDI 2017].

The numerical results of turbulent flow simulations in geometric configurations carried out at different bends [RUDOLF, DESOVA 2007]. The result was getting the coefficient of *hL* smallest at the U-bend, and the most significant at the S-bend with one large whirlpool originating and the flow marked by a considerable difference of velocity in the radial direction. The final result concluded that the flow recovery process is rather slow to reach more than 40*D* behind the last bend.

While in other research, the head loss decreases with increasing pipe diameter and increases when velocity or discharge rises regardless of pipe size [NTENGWE *et al.* 2015]. Head loss in and out of bends increases with increasing the flows and decreasing pipe diameter. Based on these conditions, the design can be chosen with the pipe diameter or connection and flow to balance the characteristics for optimal operating conditions.

Fluid flow in curved pipes with a large curvature ratio (*R*:*D*) makes internal flows more complicated [WANG *et al.* 2015]:

1) small *R:D*, θ = 30°–60°, pressure are relatively stable; the *R:D* has a more significant impact on pressure distribution, especially the inner side;
2) centrifugal force influences the pressure distribution of the upstream and downstream pipes;
3) pressure fluctuations slowly weakened;
4) as the *R:D* increases, the peak pressure gradient θ = 30°, and the separation boundary clearer after θ = 60°;
5) for curved bends with a large *R:D*, irregular internal currents.

Analysis of laminar flow at α = 90° bend pipe with a linear outlet, the conclusions obtained from the study are [PANTOKRATORAS 2016]:

1) if the *R* bend is large, the velocity profile in the inlet pipe bend to the inner wall, while at low *R*, the velocity profile remains symmetrical, and the flow through the bend does not change;
2) if the large *R* exits steeply, the velocity profile shifts to the outer wall when the Re is high, and towards the inner wall when Re is low; if *R* is small, all speed profiles shift towards the outer wall of the bend;
3) if *R* is large, the maximum velocity profile along the pipe exits, and minimum in downstream of bend when the Re is low, and *R*:*D* is small;
4) distortion formed on the downstream of bend and disappearing as it away from the bend.

The developing model in this research is a combination of effect factors of head loss at the bend. The bend model has various pieces of slices, considering the effectiveness and efficiency of the application in the field. Referring to the previous reference, the results of the analysis show non-uniformity. The results of identification obtained is various, and almost all studies focus on the curved bend, so this subject needs further analysis to obtain a new equation model that is closer.

MATERIAL AND METHODS

SLICED BENDS 90°

The head loss of sliced bend caused by the friction of the wall (*Li*), and the angle changes of bend (α). The elements that influence are velocity (*U*) number of slices (*n*), the average length of walls (*Li*), angle changes (α), friction coefficients (*f*), gravitational acceleration (*g*), and pipes slope (*I*), and Figure 1 explain about the analysis concept.

Base on Figure 1, the pressurized pipeline used *D* (diameter), *U* (velocity), the scheme of the model as Figure 1. The bend uses a nonlinear model, the number of slices (*n*),

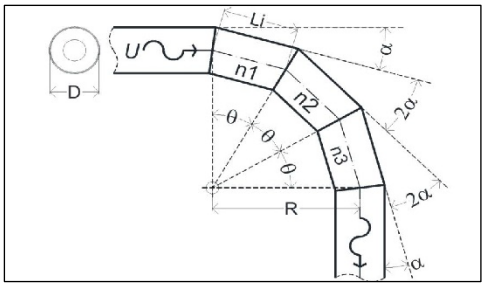

Fig. 1. Pipe with a sliced bend 90° model; *D* = diameter, *Li* = length of the linear segment, α = angle of direction change, *n* = number of slices, θ = angle slice, *R* = radius of sliced bend; source: own elaboration

the radius (R), length of the wall by Li, the direction change of flow as $n + 1$. The angle divide by the number of slices (n), and angle of change first and last is α for the upstream and downstream sections, the angle of change in the intermediate direction is 2α as $n - 1$.

The total head loss in the pipe network as passes the 90° bend is head loss due to friction and angle changes of the bend. Head loss as friction occurs between the fluid and the wall of the pipe, while the head loss is due to changes in direction because the flow angle changes suddenly on a sliced bend.

ANALYTICAL CONSIDERATIONS

Generally, the main problem that always arises in implementation when using a curved bend is time and cost in procurement. To make it easy in implementation, so the slices bend method as a choice because it can use the residual pipe. The concept was developed based on the scheme as Figure 1; the equation described by calculating the head loss coefficient that occurs using the scheme as Figure 2.

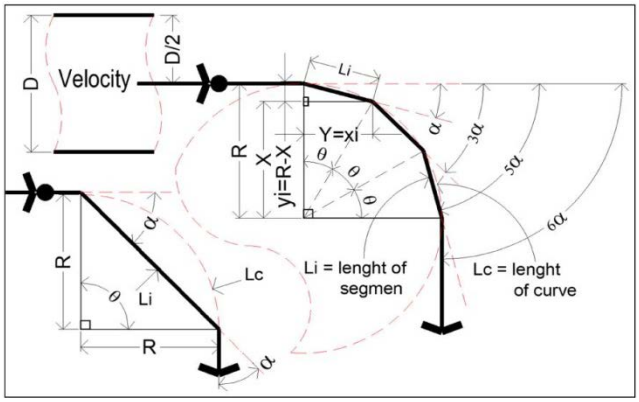

Fig. 2. Scheme of sliced bend 90° mode; D = diameter, Li = length of segment, Lc = length of curve, α = angle of direction change, θ = angle slice, R = radius of sliced bend; source: own elaboration

Figure 2 explains two kinds of slice models, with one slice and with three slices. Every section of the slice is equal segments, but the angle of bend is always different, the angle after first and before the last bend is α, but the angle between first and last bend always 2α.

Next, the number of slices $n = 3$, the equation calculate as follows:

$$X = R \cos \theta \tag{1}$$

$$Y = R \sin \theta \tag{2}$$

$$\tan \alpha = yi : xi \tag{3}$$

also,

$$\alpha = \tan^{-1} [(R - X):Y] = \tan^{-1} (yi : xi) \tag{4}$$

Length of a linear segment (Li):

$$Li = \frac{Y}{\cos \alpha} = \frac{R \sin \theta}{\cos \alpha} \tag{5}$$

the radius of sliced bend (R), angle every slice (θ), angle of direction change (α), length of the linear segment (Li), length of a curve (Lc), and the number of a slice (n).

The angle change of bends causes the flow of a slowdown, with the analytical approach of vector, angular changes as a function of the direction changes. The initial equation is the angles difference of a single bend as in Figure 2, and completely can be explained as follows:

- the angular changes formed by the sliced bend on the angle of direction change first and last are equal to α;
- the angles of change in the after first and before last of direction change angles formed equal to 2α;
- the number of slices (n) is 3 then angles α (2 points) and angles 2α (2 points), so the value of vectors is:

$$\cos^2\alpha \cdot \cos^{(n-1)} 2\alpha \tag{6}$$

- when the number of slice $n = 1$; $\cos^{(n-1)} 2\alpha = \cos^{(0)} 2\alpha = 1$, Equation (6) is: $\cos^2\alpha \cos^{(0)}2\alpha = \cos^2\alpha$.

PRIMARY POINTS

Frictions

The head loss in a sliced bend due to friction must take into account because it occurs in this research. According to the Darcy–Weisbach equation, the head loss due to friction that occurs wall along with slices of the pipe (n Li), the Equation (6) substituted in Equation (1), if the coefficient of loss due to friction denoted as δ_a the equation becomes:

$Li = \frac{Y}{\cos \alpha} = \frac{R \sin \theta}{\cos \alpha}$ substitution to; $\delta_a = f \frac{L}{D}$ so the equation is:

$$\delta_a = f \frac{L}{D} = f \frac{Li}{D} = f \frac{R \sin \theta}{D \cos \alpha} \tag{7}$$

If the sum of slices more than 1 or $n > 1$, the equation is:

$$\delta_a = f \frac{n R \sin \theta}{D \cos \alpha} \tag{8}$$

The coefficient of friction (f) as Equation (8) and the value of the Reynold number (Re) used to get the coefficient friction value. Then the value of friction coefficient (f) acc. to NAKAYAMA and BOUCHER [1998].

Flow direction changes

The head loss, which is caused by flow direction change, is accumulated in the angle change suddenly in sliced bend. The accumulation of flow direction changes that occur due to changes in angle suddenly is the accumulate of the angular changes suddenly that occur in sliced bend.

To find out of the coefficient value total of head loss due to direction changes of flow can use the Equation (6), initial flow in upstream of the sliced bend still 100%, and after downstream of the sliced bend, the flow is not 100% anymore. Furthermore, the flow direction change coefficient denoted as δ_b, and then the equation is:

$$\delta_b = 1 - (\cos^2\alpha \cdot \cos^{(n-1)} 2\alpha) \tag{9}$$

Equation (7) is an upstream flow value (100%) and then due to accumulative of angle change suddenly in sliced bend, so the coefficient becomes Equation (9).

EQUATION OF HEAD LOSS

The head loss in a sliced bend usually becomes by the friction of pipe wall and direction change of the flow. The combination of friction coefficients and coefficient of direction change of the flow are total head loss in sliced bend. If *Kb* is the total loss coefficient in sliced bend, so the final value is Equation (8) + Equation (9), and the value of *Kb* is:

$$K_b = \delta_a + \delta_b = f\frac{n\ R\sin\theta}{D\cos\alpha} + [1 - (\cos^2\alpha \cdot \cos^{(n-1)}2\alpha)] \quad (10)$$

So the head loss of the sliced bend becomes:

$$hL = K_b \frac{U^2}{2g} =$$

$$= \left[f\frac{n\ R\sin\theta}{D\cos\alpha} + [1 - (\cos^2\alpha \cdot \cos^{(n-1)}2\alpha)]\right]\frac{U^2}{2g} \quad (11)$$

For example:
The sliced bend model of 90° from a pressurized pipeline $n = 3$ surrounded by water (25°C, ε = 0.0000089 kg·cm^{-1}·s^{-1}) discharge Q = 0.50 dm^3·s^{-1}, diameter D = 5/8", 3/4", 1", 5/4" and 6/4", radius of bend $R = 2D$, if Re > 4000 then $f = \frac{0.316}{Re^{0.25}}$ calculate:

a) the head loss *hL* on the bend,
b) the head loss used to 1" diameter of pipe and number of slices n = 2, with velocity of flow U 10 m·s^{-1}, please calculate by the Ansys simulation and by Equation (11).

RESULTS

Result a) Pressurized pipes with a diameter of 5/8" = 1.59 cm so that R = 3.18 cm. Discharge 0.50 dm^3·s^{-1}. Pipe cross sectional area A = 1.98 cm^2, so the velocity U = 252.74 cm·s^{-1}. Tested with a friction coefficient f = 0.00386 then the Reynolds number (Re) = 45.081·10^6 > 4000 (yes), then with the number of slices n = 3 pieces, the angle θ = 30° and α = 15°, with the Equation (11) the value of δ_a = 0.01240 and δ_b = 0.30007 then *Kb* = 0.31247, with a diameter of pipe 5/8" with a discharge 0.50 dm^3·s^{-1}, *hL* = 10.17 cm. In succession with *D* above, the full value is obtained as following Table 1.

According to the calculation method, the discharge Q is 0.01 to 0.65 dm^3·s^{-1}, then the discharge and the head loss 90° sliced bend with n = 3, as shown in Figure 3.

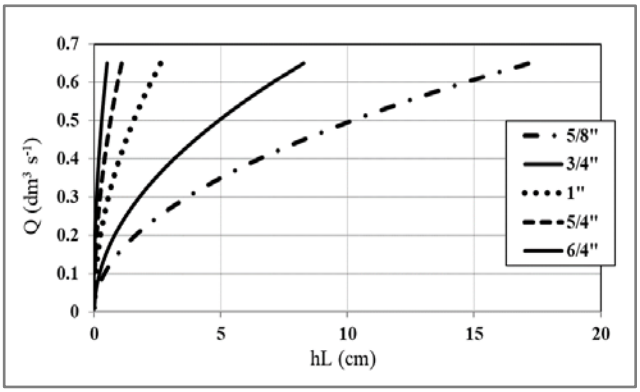

Fig. 3. Relationship between discharge Q and head loss *hL* (n = 3, $R : D$ = 2) with Equation 11; source: own study

Result b) Pressurized pipes with a diameter of 1" = 2.54 cm, R = 5.08 cm. Pipe cross-sectional area A = 5.06 cm^2, and then the velocity U = 10 m·s^{-1}. Tested with a friction coefficient f = 0.00243 then the Reynolds number Re = 285.393·10^6 > 4000, used the number of slices (n) 2 pieces, the angle θ and α depend on n, according to the Equation (11) the value of δ_a = 0.00806 and δ_b = 0.39644 then *Kb* = 0.40450, the *hL* = 206.17 cm.

The simulations of flow by Ansys, providing 10 m·s^{-1} initial velocity with 25.4 mm diameter of the pipe and used the variation of slices (n) = 2. While the pressure at upstream of bend in this simulation is 4.371·10^4 Pa, and pressure at downstream of the bend is 3.182·10^4 Pa. So, the pressure drop at the sliced bend with the variation of slices n = 2 is equal to 1.189·10^4 Pa = 0.1189 bar or *hL* = 121.24 cm, and normal flow at 22*D* after the sliced bend.

Data verification. Verify the analysis results obtained using Ansys simulations or simulation models in the laboratory. In this study, verify the results of the analysis using Ansys simulations and full-scale models in the laboratory. In the example of the previous sub-chapter, the results of the analysis of the computation of the *hL* calculation have been verified based on Equation (10) and compared with the simulation of Ansys with a flow velocity of 10 m·s^{-1} in a sliced bend with n = 2 and a diameter of 25.4 mm.

Then verification is also carried out by comparing the full-scale model in the laboratory with various variations of discharge and variation of slices bend from n = 1 to n = 5. The purpose of verification, find out the results of the equation, whether or not the trend formed by a full-scale model simulation in a laboratory is corresponding or not.

Table 1. Head loss of sliced bend 90° by equation 8 and 9 with n = 3

Parameter	Unit	90° sliced bend (n = 3)				
Pipe diameter (D)	inch	5/8"	3/4"	1"	5/4"	6/4"
Discharge (Q)	dm^3·s^{-1}	0.50	0.50	0.50	0.50	0.50
Friction (δ_a)[1)]	–	0.01240	0.01298	0.01395	0.01475	0.01543
Direction change (δ_b)[2)]	–	0.30007	0.30007	0.30007	0.30007	0.30007
Coefficient of head loss (K_b) = (δ_a + δ_b)	–	0.31247	0.31298	0.31402	0.31482	0.31550
Head loss (hL)[3)]	cm	10.17862	4.91775	1.56082	0.64094	0.30977

[1)] Equation (8); [2)] Equation (9); [3)] Equation (11).
Source: own study.

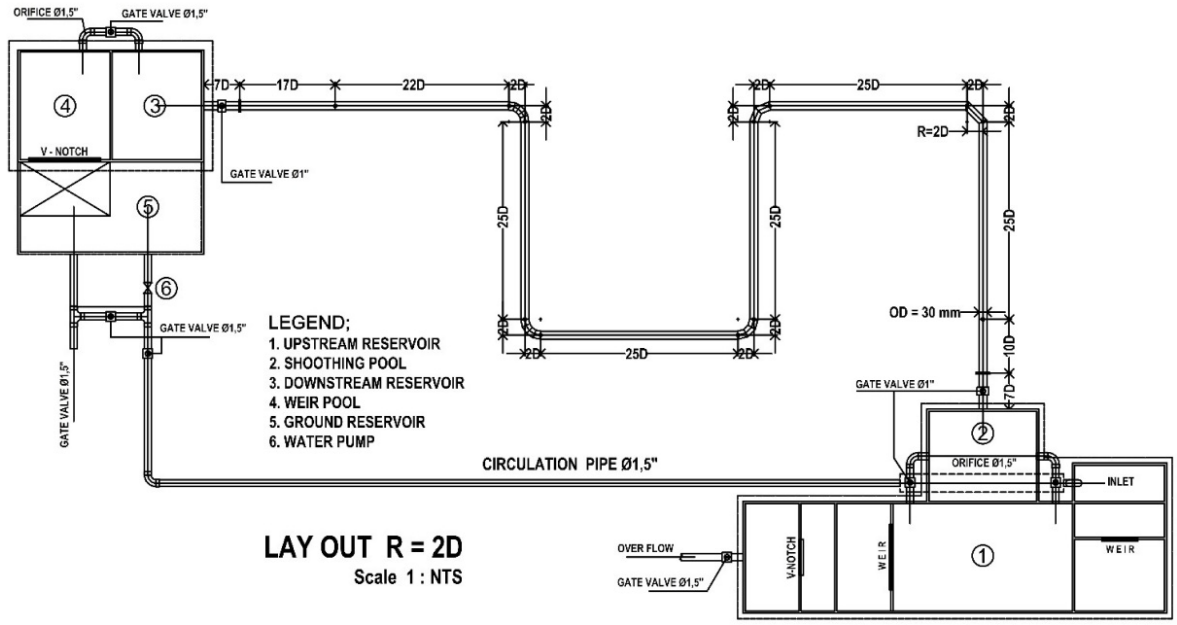

Fig. 4. Full-scale scheme model of sliced bend 90°; source: own elaboration

Scheme/plan of the full-scale model is shown in Figure 4. The full-scale isometric model in the laboratory and the originated primary data collected is illustrated in Photo 1. Figure 5 is 3D simulations of flow in sliced bend 90° by Ansys with 25,4 mm of diameter, n = 2, and velocity of flow $U = 10\ \mathrm{m \cdot s^{-1}}$.

Based on the analysis of Equation (11), the value of *hL* obtained was 206.17 cm, while the value of *hL* obtained based on Ansys simulation was 41% lower than Equation (11), which was 121.24 cm. Overall the flow profile shown in the Ansys simulation shows turbulence before entering the bend. Then the flow returns to normal is reached after leaving the bend as far as 22*D*. The behaviour of flow could saw in Figure 5.

Then the simulations of Equation (11) (eq) with a full-scale model (fcm), varying the number of slices with n = 1 to n = 5, discharge variations starting from 0.01 $\mathrm{dm^3 \cdot s^{-1}}$ at bends with curvature ratio R:D = 2 and 25.4 mm diameter pipes are as shown in Table 2. Table 2 presents the results of the analysis of Equation (11) with variations in the number of slices of 5 and flow rate variants of 14 treatments the results of full-scale model measurements in the laboratory with variations in the number of slices equal to Equation (11) and flowrate of 10 treatments.

The results are as shown in Figure 6. A comparison of the results of the analysis of Equation (11) at n = 1, with a full-scale model with the number of slices n = 1 is shown in Figure 6a. The graph of *hL* values in the comparison shows an identical trend, but the value of *hL* in Equation (11) is smaller than the results of *hL* on a full-scale model.

In Figure 6b, a comparison of the results of *hL* at n = 2 between the results of the analysis of Equation (11) with the full-scale model, the trends formed are identical and coincide, showing that the graphs of the results of the formed *hL* are aligned and identical. An identical trend is shown in Figure 6c–e even though the value of *hL* generated is even further away, meaning that it has a significantly different yield value.

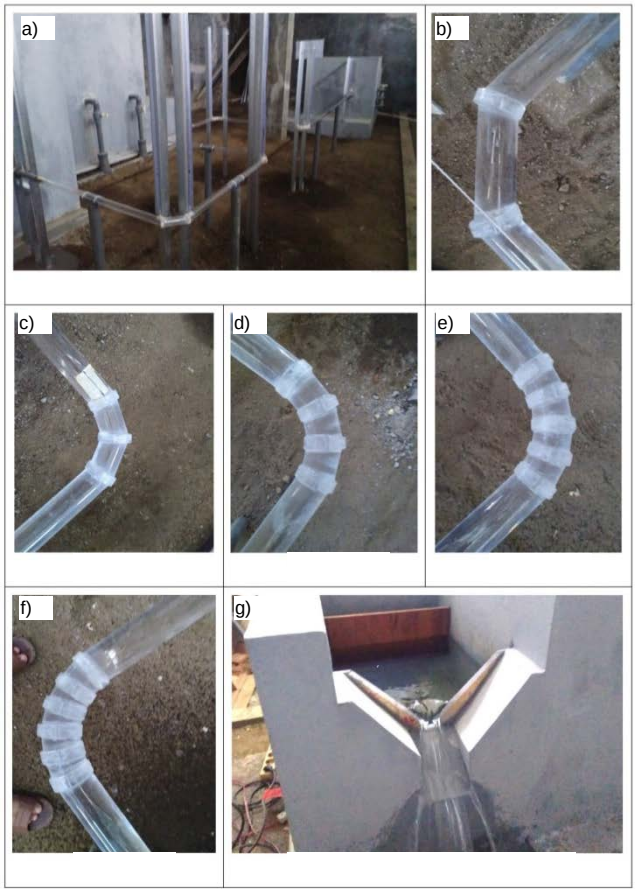

Photo 1. Full-scale model of sliced bend 90° (R:D = 2); a) full-scale model of sliced bend 90°, b) n1 model, c) n2 model, d) n3 model, e) n4 model, f) n5 model, g) V-notch downstream control (phot. *M. Abduh*)

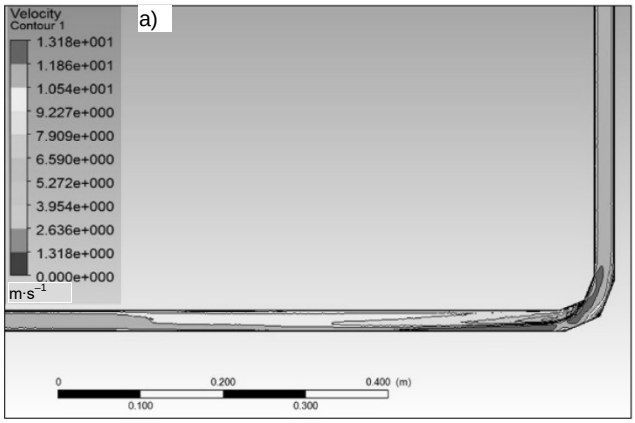
a)
Velocity
Contour 1
1.318e+001
1.186e+001
1.054e+001
9.227e+000
7.909e+000
6.590e+000
5.272e+000
3.954e+000
2.636e+000
1.318e+000
0.000e+000
m·s⁻¹
0
0.200
0.400 (m)
0.100
0.300

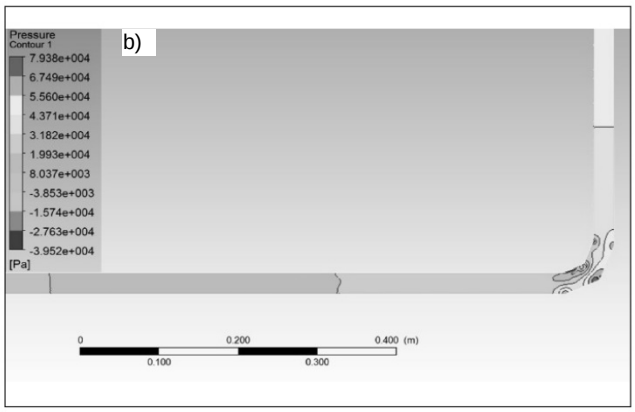
b)
Pressure
Contour 1
7.938e+004
6.749e+004
5.560e+004
4.371e+004
3.182e+004
1.993e+004
8.037e+003
-3.853e+003
-1.574e+004
-2.763e+004
-3.952e+004
[Pa]
0
0.200
0.400 (m)
0.100
0.300

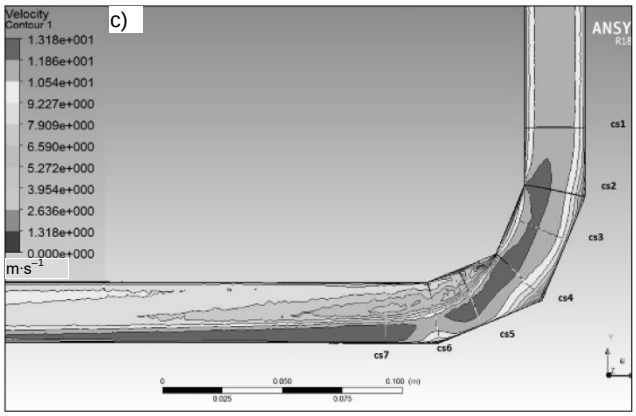
c)
Velocity
Contour 1
1.318e+001
1.186e+001
1.054e+001
9.227e+000
7.909e+000
6.590e+000
5.272e+000
3.954e+000
2.636e+000
1.318e+000
0.000e+000
m·s⁻¹
ANSY
cs1
cs2
cs3
cs4
cs5
cs6
cs7

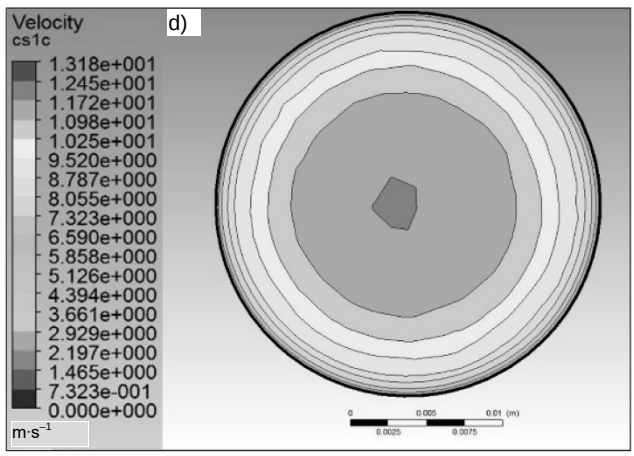
d)
Velocity
cs1c
1.318e+001
1.245e+001
1.172e+001
1.098e+001
1.025e+001
9.520e+000
8.787e+000
8.055e+000
7.323e+000
6.590e+000
5.858e+000
5.126e+000
4.394e+000
3.661e+000
2.929e+000
2.197e+000
1.465e+000
7.323e-001
0.000e+000
m·s⁻¹

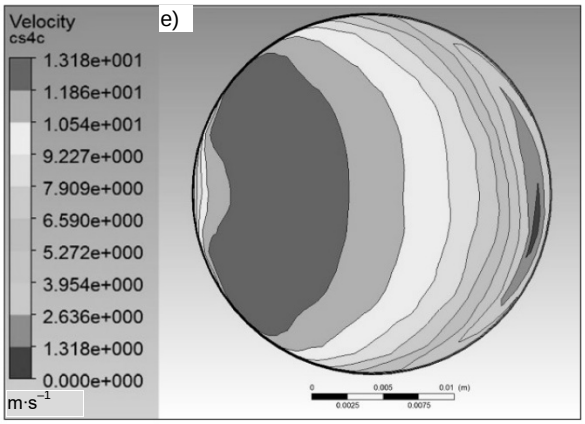
e)
Velocity
cs4c
1.318e+001
1.186e+001
1.054e+001
9.227e+000
7.909e+000
6.590e+000
5.272e+000
3.954e+000
2.636e+000
1.318e+000
0.000e+000
m·s⁻¹

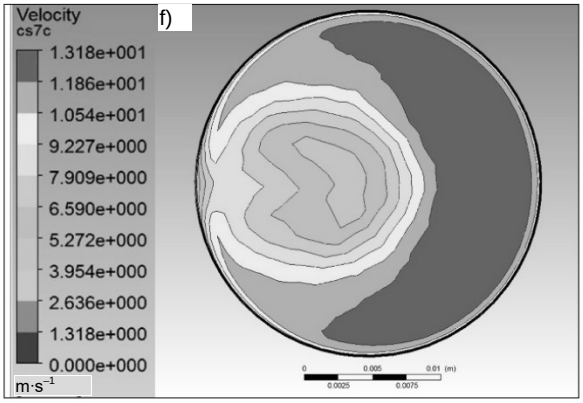
f)
Velocity
cs7c
1.318e+001
1.186e+001
1.054e+001
9.227e+000
7.909e+000
6.590e+000
5.272e+000
3.954e+000
2.636e+000
1.318e+000
0.000e+000
m·s⁻¹

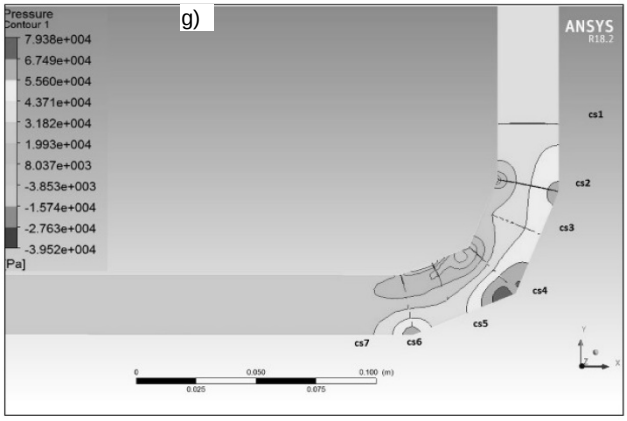
g)
Pressure
Contour 1
7.938e+004
6.749e+004
5.560e+004
4.371e+004
3.182e+004
1.993e+004
8.037e+003
-3.853e+003
-1.574e+004
-2.763e+004
-3.952e+004
Pa]
ANSYS
cs1
cs2
cs3
cs4
cs5
cs6
cs7

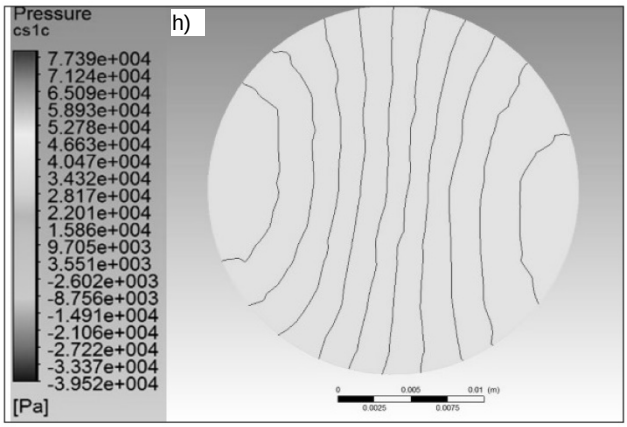
h)
Pressure
cs1c
7.739e+004
7.124e+004
6.509e+004
5.893e+004
5.278e+004
4.663e+004
4.047e+004
3.432e+004
2.817e+004
2.201e+004
1.586e+004
9.705e+003
3.551e+003
-2.602e+003
-8.756e+003
-1.491e+004
-2.106e+004
-2.722e+004
-3.337e+004
-3.952e+004
[Pa]

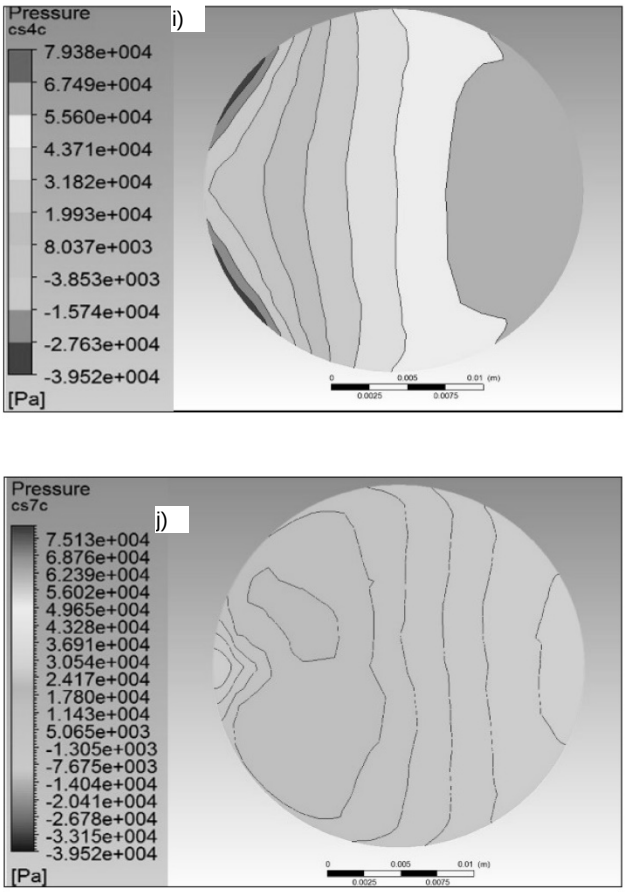

Fig. 5. The behaviour of flow and head loss of sliced bend; a) velocity contour, b) head loss contour, c) the section arrangement of *U*, d) the upstream section, e) the middle section, f) the downstream section, g) arrangement of *hL*, h) the upstream section of *hL*, i) the middle section of *hL*, j) the downstream section of *hL*; cs = cross section; source: own study

Table 2. Head loss and variation of 90° sliced bend with Equation (11) and the full-scale model

No. of treatment	Discharge ($dm^3 \cdot s^{-1}$)	Head loss (*hL*) in 90° sliced bend (cm) at number of slices (*n*)				
		1	2	3	4	5
With Equation (11)						
1	0.01	0.0011	0.0009	0.0007	0.0006	0.0005
2	0.05	0.0264	0.0210	0.0161	0.0132	0.0112
3	0.10	0.1045	0.0830	0.0638	0.0521	0.0442
4	0.15	0.2340	0.1859	0.1427	0.1163	0.0986
5	0.20	0.4148	0.3295	0.2526	0.2057	0.1742
6	0.25	0.6466	0.5136	0.3935	0.3203	0.2710
7	0.30	0.9295	0.7382	0.5653	0.4598	0.3890
8	0.35	1.2633	1.0033	0.7680	0.6244	0.5280
9	0.40	1.6480	1.3088	1.0015	0.8140	0.6881
10	0.45	2.0836	1.6546	1.2658	1.0285	0.8691
11	0.50	2.5701	2.0409	1.5608	1.2680	1.0712
12	0.55	3.1074	2.4674	1.8866	1.5323	1.2942
13	0.60	3.6954	2.9343	2.2431	1.8215	1.5381
14	0.65	4.3342	3.4414	2.6303	2.1355	1.8030
With the full-scale model						
1	0.4071	3.50	1.40	1.90	2.10	0.90
2	0.4747	5.30	2.10	2.90	3.20	1.70
3	0.6268	7.90	3.30	4.50	4.30	3.70
4	0.8023	8.80	4.60	6.50	6.70	6.40
5	0.8791	10.90	5.50	7.90	10.80	7.90
6	0.9598	15.30	7.70	11.10	10.50	10.80
7	1.0015	17.00	8.80	11.80	11.90	11.90
8	1.0443	19.60	10.20	13.80	13.90	14.30
9	1.1102	22.80	11.70	16.10	15.90	16.40
10	1.1327	24.00	12.40	16.80	17.00	18.40

Source: own study.

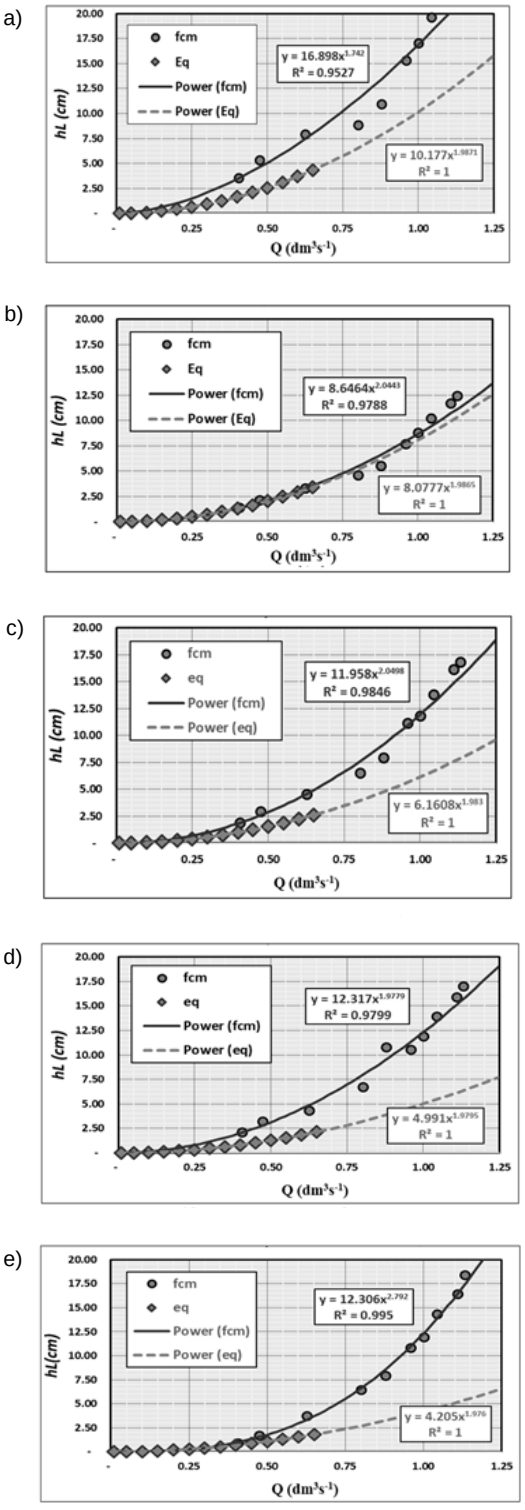

Fig. 6. Relationship between *Q* and *hL* of sliced bend 90°: a) *n* = 1, b) *n* = 2, c) *n* = 3, d) *n* = 4, e) *n* = 5; *Q* = $dm^3 \cdot s^{-1}$, *R:D* = 2, *D* = 25.4 mm; fcm = full-scale model, eq = Equation (11); source: own study

The measurement of flow discharge on a pipe based on the flow passing through the triangle threshold (V-notch) at the downstream of the test model. The trends that formed for overall compressive height loss are relatively identical, although there are still differences in results (Fig. 7).

No.	Q (dm³s⁻¹)	h (cm)
1	0.00343	0.80
2	0.01796	1.10
3	0.03864	1.40
4	0.08961	1.70
5	0.11491	2.00
6	0.07719	2.30
7	0.14963	2.60
8	0.20563	2.90
9	0.34550	3.20
10	0.39367	3.50
11	0.40457	3.80
12	0.52083	4.10
13	0.70150	4.70
14	0.87181	5.00
15	1.00443	5.30
16	1.06249	5.60

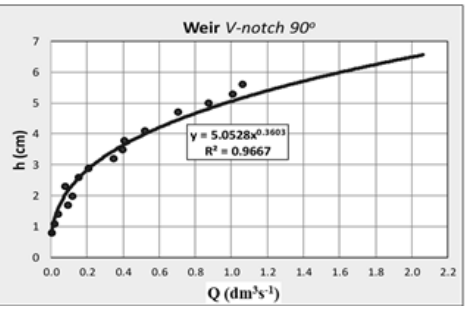

Fig. 7. Discharge *Q* validation of weir V-notch 90°; source: own study

DISCUSSION

Overall the results of the analysis of Equation (11) show a trend that is identical to the full-scale model, and from these graphs illustrates that Equation (11) is corresponding the hypothesis used in this study. The value of *hL* obtained from the analysis of Equation (11) is all below the *hL* value of the full-scale model. It caused by several factors, including the accuracy in reading full-scale model measurements, especially the stability of the upstream water level during data collection and the addition of the coefficient in Equation (11).

Based on the condition above, the results obtained from the Ansys simulation also further away from the *hL* values obtained from the full-scale model. There are still too many things that need to be further investigated concerning the flow phenomenon at the 90° slice bend to be studied.

Based on the results above, the measurements on the full-scale model must be more carefully, especially the time of measurement, the water surface conditions at the upstream of the model must be stable, so that the difference of head loss and water level of the downstream tank is also stable.

In the simulation of Equation (11), necessary to correct the number for the head loss coefficient obtained, especially for the number of slices $n = 1$ and $n > 2$, because the number of slices has a significant difference compared to the measurement results on the full-scale model. For the number of slices $n = 1$ and $n > 2$, there needs to be a correction value on the equation of the head loss coefficient.

Further research needs to do so the head loss equation that getting is more identical to the head loss coefficient based on a full-scale model.

CONCLUSIONS

The head loss equation at sliced bend 90° is a combination of friction and direction changes inflow at the sliced bend. This method chose because expected to provide convenience, fast, and economical to implement. Elements that influence are the velocity of flow, the number of sliced, the average length of sliced walls, angle changes of the sliced, coefficient of friction, acceleration of gravity, and slope of the pipe. Equation (11) is an analysis method for calculating the coefficient of *hL*.

The results of the analysis based on Equations (11). If the larger diameter of the pipe and the more slices with a fixed discharge, the coefficient of head loss becomes small. Conversely, if the diameter of the pipe is getting smaller, and the slice is getting less, then the coefficient of head loss becomes bigger. The method aims to give new knowledge in pipeline network applications, especially for the big diameter of pipelines, and the plan of the *hL*, cost, and time could be more effective.

According to the hypothesis used, could conclude that the trends obtained from these equations showed the relevant results and provided an identical picture when applied to pipe networks to facilitate implementation, time efficiency and can reduce costs incurred in implementation.

The results of the analysis of Equation (11) with the number of slices $n = 2$ have the most identical values to the results of full-scale model measurements. It means that the equation approaches the real state, while for the number of slices or *n*1, *n*3, *n*4, and *n*5 are trending following the full-scale model, but the value of *hL* is lower than the full-scale model. As for the Ansys simulation, the resulting *hL* value is lower than Equation (11). Based on the results of this study, further research needed to obtain broader results related to the flow phenomenon at the slice bend, including the effect of flow on the condition of the pipe material.

ACKNOWLEDGMENTS

This research, supported by the Universitas Muhammadiyah Malang (UMM), as an institution of place the writer in charge, has provided the facilities needed during this research and all parties who have participated in completing this research.

REFERENCES

ADJEI R.A., MOHSIN A. 2014. Simulation-driven design optimization: A case study on a double 90 degree elbow bend. International Journal of Modeling and Optimization. Vol. 4. Iss. 6 p. 426–432. DOI 10.7763/IJMO.2014.V4.412.

CHOWDHURY R.R., ALAM M.M., SADRUL ISLAM A.K.M. 2016. Numerical modeling of turbulent flow through bend pipes [online]. Mechanical Engineering Research Journal. Vol. 10 p. 14–19. [Access 25.10.2019]. Available at: http://www.cuet.ac.bd/merj/vol.10/MERJ-03.pdf

DUTTA P., NANDI N. 2015a. Effect of Reynolds number and curvature ratio on single phase turbulent flow in pipe bends [online]. Mechanics and Mechanical Engineering. Vol. 19. Iss. 1 p. 5–16. [Access 25.10.2019]. Available at: https://www.researchgate.net/publication/282884519_Effect_of_Reynolds_number_and_curvature_ratio_on_single_phase_turbulent_flow_in_pipe_bends

DUTTA P., NANDI N. 2015b. Study on pressure drop characteristics of single phase turbulent flow in pipe bend for high Reynolds number [online]. ARPN – Journal of Engineering and Applied Sciences. Vol. 10. Iss. 5 p. 2221–2226. [Access 25.10.2019]. Available at: https://www.researchgate.net/publication/282716633_Study_on_pressure_drop_characteristics_of_single_phase_turbulent_flow_in_pipe_bend_for_high_reynolds_number

DUTTA P., SAHA S.K., NANDI N., PAL N. 2016. Engineering science and technology, an international journal numerical study on flow separation in 90° pipe bend under high Reynolds number by k-ε modeling. Engineering Science and Technology, an International Journal. Vol. 19(2) p. 904–910. DOI 10.1016/j.jestch.2015.12.005.

HELLSTRÖM L. H.O., ZLATINOV M.B., CAO G., SMITS A.J. 2013. Turbulent pipe flow downstream of a 90-degree bend. Journal Fluids Mechanics. Vol. 735. R7 p. 1–12. DOI 10.1017/jfm.2013.534.

ISLAM M.S., BASAK A., SARKAR M.A.R., ISLAM M.Q. 2016. Study of minor loss coefficient of flexible pipes [online]. Global Journal of Research in Engineering : A Mechanical and Mechanical Engineering. Vol. 16. Iss. 4 p. 27–32. [Access 25.10.2019]. Available at: https://globaljournals.org/GJRE_Volume16/3-Study-of-Minor-Loss-Coefficient.pdf

KIM J., YADAV M., KIM S. 2014. Characteristics of secondary flow induced by 90- degree elbow in turbulent pipe flow. Engineering Applications of Computational Fluid Mechanics. Vol. 8. Iss. 2 p. 229–239. DOI 10.1080/19942060.2014.11015509.

KUMAR SAHA S.., NANDI N. 2017. Change in flow separation and velocity distribution due to effect of guide vane installed in a 90 [online]. Mechanics and Mechanical Engineering. Vol. 21. Iss. 2 p. 353–361. [Access 25.10.2019]. Available at: http://www.kdm.p.lodz.pl/articles/2017/21_2_12.pdf

LU X., LI B., HUANG L., ZHENG W., LIU J., WANG L. 2015. The establishment and verification of 90° elbow pipe with circular cross section internal pressure distribution model [online]. In: 5th International Conference on Advanced Design and Manufacturing Engineering (ICADME 2015) p. 1836–1839. [Access 25.10.2019]. Available at: https://download.atlantis-press.com/article/25840416.pdf

NAKAYAMA Y., BOUCHER R.F. 1998. Introduction to fluid mechanics. Woburn, MA. Butterworth-Heinemann. ISBN 978-0-340-67649-3 pp. 322.

NOORANI A., SARDINA G., BRANDT L., SCHLATTER P. 2015. Particle velocity and acceleration in turbulent bent pipe flows. Flow, Turbulence and Combustion. Vol. 21 p. 539–559. DOI 10.1007/s10494-015-9638-9.

NTENGWE F.W., CHIKWA M., WITIKA L.K. 2015. Evaluation of friction losses in pipes and fittings of process engineering plants [online]. International Journal of Scientific and Technology Research. Vol. 4. Iss. 10 p. 330–336. [Access 25.10.2019]. Available at: http://www.ijstr.org/final-print/oct2015/Evaluation-Of-Friction-Losses-In-Pipes-And-Fittings-Of-Process-Engineering-Plants.pdf

PANTOKRATORAS A. 2016. Steady laminar flow in a 90° bend. Advances in Mechanical Engineering. Vol. 8. Iss. 9 p. 1–9. DOI 10.1177/1687814016669472.

RUDOLF P., DESOVA M. 2007. Flow characteristics of curved ducts [online]. Applied and Computational Mechanics. No. 1 (October 2007) p. 255–264. [Access 25.10.2019]. Available at: https://www.kme.zcu.cz/acm/old_acm/full_papers/acm_vol1no1_p029.pdf

SPEDDING P.L., BENARD E., MCNALLY G.M. 2008. Fluid flow through 90-degree bends. Asia-Pacific Journal of Chemical Engineering. Vol. 12 p. 107–128. DOI 10.1002/apj.5500120109.

SUMIDA M., SENOO T. 2015. Experimental investigation on pulsating flow in a bend. Proceedings of the International Proceedings of the International Conference on Heat Transfer and Fluid Flow. Vol. 27. Iss. 82 p. 26–33. DOI 10.11159/jffhmt.2015.004.

WAHYUDI S., SOEPARMAN S., SOENOKO R., YUNIZAR R.A. 2016. Characteristics of two-phase fluid flow in pipe bends [online]. ARPN Journal of Engineering and Applied Sciences. Vol. 11. Iss. 4 p. 794–798. [Access 25.10.2019]. Available at: http://www.arpnjournals.org/jeas/research_papers/rp_2016/jeas_0216_3723.pdf

WANG S., REN CH., SUN Y., YANG X., JIYUAN T. 2016. A study on the instantaneous turbulent flow field in a 90-degree elbow pipe with circular section. Science and Technology of Nuclear Installations. Vol. 2016. ID 5265748. DOI 10.1155/2016/5265748.

WANG Y., DONG Q., WANG P. 2015. Numerical investigation on fluid flow in a 90-degree curved pipe with large curvature ratio. Mathematical Problems in Engineering. Vol. 2015 (July 27, 2015). Art. ID 548262 p. 1–12. DOI 10.1155/2015/548262.

ZEGHADNIA L., DJEMILI L., HOUICHI L., NORDINE R. 2015. Efficiency of the flow in the circular pipe. Journal of Environmental Science and Technology. Vol. 8. Iss. 2 p. 42–58. DOI 10.3923/jest.2015.42.58.

ZHANG S., SU B., LIU J., LIU X., QI G., GE Y. 2018. Analysis of flow characteristics and flow measurement accuracy of the elbow with different diameters. In: IOP Conference Series: Earth and Environmental Science. IOP Publishing, 9. DOI 10.1088/1755-1315/113/1/012231.